# PDE State Observers for Lithium-Ion Batteries Considering Temperature Effects

Sara Sepasiahooyi[1] and Shu-Xia Tang[2]

***Abstract*— Precise estimation of the electrochemical states of a Li-ion battery benefits the design of a more efficient and reliable battery monitoring system. This paper explores state estimation approaches for a Single Particle Model with electrolyte (SPMe) dynamics with modified boundary conditions integrated into a Thermal model (SPMe-T). The integration of thermal dynamics into the SPMe enhances its capability to capture temperature-dependent behavior, while maintaining a balanced trade-off between computational efficiency. An internal average temperature model is incorporated into the battery model to account for temperature variations that affect the diffusion parameter. Battery parameters, such as the diffusion coefficient, vary with temperature. Incorporating a thermal model can improve subsequent state estimation. This study estimates the lithium concentration in both the electrolyte and solid phases by proposing closed-loop backstepping Partial Differential Equation (PDE) observers. The stability of all proposed observers and the convergence of the state estimation errors are proven.**

## I. INTRODUCTION

Proper monitoring of lithium-ion batteries is essential to maintain their longevity and manage undesired conditions; otherwise, it can lead to various adverse consequences, ranging from accelerated aging to hazardous faults [1]. Although the electrolyte plays a critical role in facilitating lithium-ion transport and interfacial electrochemical reactions within lithium-ion batteries, its dynamics and behavior have been relatively less explored compared to the solid-phase dynamics. Most state estimation studies in the literature have focused primarily on the solid phase. For instance, in [2], Moura et al. employed the SPM and designed backstepping PDE observers to estimate the lithium concentration in the solid phase. In [3], temperature effects on battery parameters were considered, and a thermal–electrochemical model was used to estimate the solid-phase lithium concentration, followed by the estimation of the state of charge. Regarding the electrolyte phase, in [4], an open-loop observer was designed to estimate the lithium concentration in the electrolyte. In [5], the open-loop observer in [4] was further developed, and closed-loop PDE observers for electrolyte concentration were designed by incorporating the boundary error as a correction term. In this design, the temperature was assumed to be constant. Since battery parameters are influenced by temperature, considering thermal effects in state estimation can improve performance. In the present study, the effect of temperature on the system parameters is taken into account. Accordingly, this study utilizes the SPMe-T model to capture the influence of temperature on the battery's electrochemical parameters. By integrating an internal average temperature model into the SPMe, the effect of temperature on the diffusion coefficient is captured, and closed-loop backstepping PDE observers are subsequently designed to estimate the battery states.

The main contributions of this study are as follows:

- In [5], the authors designed closed-loop backstepping PDE observers to estimate the electrolyte lithium concentration while ignoring temperature effects. To the best of our knowledge, this is the first paper in which the electrolyte-phase lithium concentration is estimated while accounting for the influence of temperature on the battery parameters.
- In [3], the SPM-T model was utilized for solid-phase state estimation. In this study, a more comprehensive model, SPMe-T with modified boundary conditions, is employed as an enhanced version of SPM-T that incorporates electrolyte-phase dynamics and temperature effects into the battery model. It also allows the diffusion coefficient in both the solid and electrolyte phases to vary with temperature.
- For the observer design in this paper, the governing PDEs are directly utilized, avoiding spatial discretization, unlike studies that rely on discretization-based approaches [6].
- Unlike the design in [5], where the boundary conditions of the target system for the electrolyte observers are set to zero, this study introduces a novel aspect by defining nonzero boundary conditions. This modification prevents the observer gain from becoming zero.

The rest of this paper is organized as follows. Section II describes the battery model. Sections III and IV present the designed observers for the electrolyte and solid phases, respectively. Finally, Section V concludes the paper and outlines directions for future work.

## II. SPMe-T MODEL

The battery model, SPMe, depicted in Fig. 1, is integrated with a thermal model to account for temperature effects. The resulting coupled model, referred to as SPMe-T, is employed as the battery model in this study and is described in the following section.

[1]Sara Sepasiahooyi, Department of Mechanical and Aerospace Engineering, Texas Tech University, Lubbock, TX 79409, USA ssepasia@ttu.edu

[2]Shu-Xia Tang, Department of Mechanical and Aerospace Engineering, Texas Tech University, Lubbock, TX 79409, USA shuxia.tang@ttu.edu

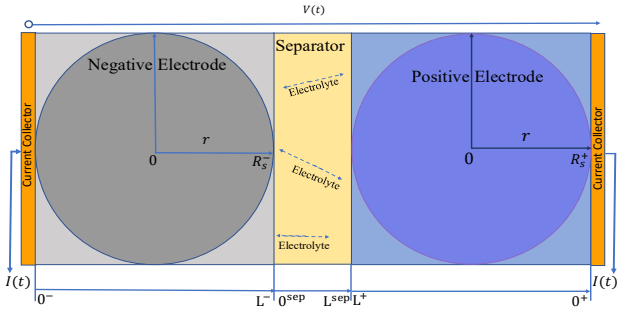


Fig. 1. SPMe Schematic

### A. Solid-phase lithium concentration

Lithium concentration in the positive and negative electrodes $c_{\mathrm{s}}^{\pm}(t,r)$ is described as:

$$\frac{\partial c_{\mathrm{s}}^{\pm}}{\partial t}(t,r) = \frac{1}{r^2}\frac{\partial}{\partial r}\left[D_{\mathrm{s}}^{\pm}(T(t))\, r^2 \frac{\partial c_{\mathrm{s}}^{\pm}}{\partial r}(t,r)\right], \quad t>0,\ r\in(0,R_{\mathrm{s}}^{\pm}), \tag{1}$$

$$\frac{\partial c_{\mathrm{s}}^{\pm}}{\partial r}(t,0) = 0,\ t\geq 0, \tag{2}$$

$$\frac{\partial c_{\mathrm{s}}^{\pm}}{\partial r}\left(t,R_{\mathrm{s}}^{\pm}\right) = \pm\frac{1}{D_{\mathrm{s}}^{\pm}(T(t))Fa_{\mathrm{s}}^{\pm}L^{\pm}}I(t),\ t\geq 0, \tag{3}$$

$$c_{\mathrm{s}}^{\pm}(0,r) = c_{\mathrm{s},0}^{\pm}(r),\ r\in[0,R_{\mathrm{s}}^{\pm}]. \tag{4}$$

Here $R_{\mathrm{s}}^{\pm}$, $F$, and $L^{\pm}$ are the particle radius, Faraday's constant, and electrode length, respectively. $a_{\mathrm{s}}^{\pm}$ is the interfacial surface area. $D_{\mathrm{s}}^{\pm}(T(t))$ is Arrhenius-like in the internal averaged temperature $T(t)$ [7]:

$$D_{\mathrm{s}}^{\pm}(T(t)) = D_{\mathrm{s}}^{\pm}(T(0))\, e^{E_{D_{\mathrm{s}}^{\pm}}\frac{T(t)-T(0)}{T(t)T(0)}}, \tag{5}$$

where $E_{D_{\mathrm{s}}^{\pm}}$ is the activation energy coefficient for solid-phase diffusivity. The internal average temperature, denoted by $T(t)$, is introduced in Section II-D.

### B. Electrolyte-phase lithium concentration

The electrolyte concentrations in the negative electrode, separator, and positive electrode are given as follows:

$$\frac{\partial c_{\mathrm{e}}^{-}}{\partial t}(t,x) = \frac{D_{\mathrm{e}}^{-,\mathrm{eff}}(T(t))}{\varepsilon_{\mathrm{e}}^{-}}\frac{\partial^2 c_{\mathrm{e}}^{-}}{\partial x^2}(t,x) + \frac{(1-t_c^0)}{\varepsilon_{\mathrm{e}}^{-}FL^{-}}I(t), \tag{6}$$

$$\frac{\partial c_{\mathrm{e}}^{\mathrm{sep}}}{\partial t}(t,x) = \frac{\partial}{\partial x}\left[\frac{D_{\mathrm{e}}^{\mathrm{sep,eff}}(T(t))}{\varepsilon_{\mathrm{e}}^{\mathrm{sep}}}\frac{\partial c_{\mathrm{e}}^{\mathrm{sep}}}{\partial x}(t,x)\right], \tag{7}$$

$$\frac{\partial c_{\mathrm{e}}^{+}}{\partial t}(t,x) = \frac{D_{\mathrm{e}}^{+,\mathrm{eff}}(T(t))}{\varepsilon_{\mathrm{e}}^{+}}\frac{\partial^2 c_{\mathrm{e}}^{+}}{\partial x^2}(t,x) + \frac{(1-t_c^0)}{\varepsilon_{\mathrm{e}}^{+}FL^{+}}I(t). \tag{8}$$

The electrolyte lithium concentration has coupled boundary conditions at the separator–electrode interfaces, which makes observer design challenging. Therefore, modified boundary conditions are used in these areas, as described in [8].

$$\frac{\partial c_{\mathrm{e}}^{\pm}}{\partial x}(t,0^{\pm}) = 0, \tag{9}$$

$$\frac{\partial c_{\mathrm{e}}^{-}}{\partial x}(t,L^{-}) = \frac{\partial c_{\mathrm{e}}^{\mathrm{sep}}}{\partial x}(t,0^{\mathrm{sep}}) = \frac{-c_{\mathrm{e}}^{-}(t,L^{-})}{P^*}, \tag{10}$$

$$\frac{\partial c_{\mathrm{e}}^{+}}{\partial x}(t,L^{+}) = \frac{\partial c_{\mathrm{e}}^{\mathrm{sep}}}{\partial x}(t,L^{\mathrm{sep}}) = \frac{c_{\mathrm{e}}^{+}(t,L^{+})}{L^{\mathrm{sep}}-P^*}, \tag{11}$$

where $P^* = \frac{L^{+}+L^{\mathrm{sep}}-L^{-}}{2}$. The initial condition for the electrolyte phase is given by $c_{\mathrm{e}}^{i}(0,x) = c_{\mathrm{e},0}^{i}(x),\ \ i\in\{-,\mathrm{sep},+\}$. The electrolyte diffusivity is Arrhenius-like [9]:

$$D_{\mathrm{e}}^{i}(T(t)) = D_{\mathrm{e}}^{i}(T(0))\, e^{E_{D_{\mathrm{e}}^{i}}\frac{T(t)-T(0)}{T(t)T(0)}}, i\in\{-,\mathrm{sep},+\}, \tag{12}$$

where $E_{D_{\mathrm{e}}}^{i}$ is the activation energy coefficient in the electrolyte-phase.

### C. Input and output

The input to the system is the applied current, $I(t)$, and the output is the terminal voltage, expressed as

$$\begin{aligned} V(t) = &-\frac{RT(t)}{\alpha F}\sinh^{-1}\left(\frac{I(t)}{2a^{+}L^{+}i_0^{+}(t)}\right) \\ &-\frac{RT(t)}{\alpha F}\sinh^{-1}\left(\frac{I(t)}{2a^{-}L^{-}i_0^{-}(t)}\right) \\ &+U^{+}\left(c_{\mathrm{ss}}^{+}(t),T(t)\right)-U^{-}\left(c_{\mathrm{ss}}^{-}(t),T(t)\right) \\ &-\left(\frac{R_f^{+}}{a_{\mathrm{s}}^{+}L^{+}}+\frac{R_f^{-}}{a_{\mathrm{s}}^{-}L^{-}}\right)I(t)+\frac{L^{+}+2L^{\mathrm{sep}}+L^{-}}{2\kappa}I(t) \\ &+k_{\mathrm{conc}}\ln\left(\frac{c_{\mathrm{e}}^{+}(t,0^{+})}{c_{\mathrm{e}}^{-}(t,0^{-})}\right), \end{aligned} \tag{13}$$

where $k_{\mathrm{conc}} = \frac{2RT\left(1-t_c^0\right)}{F}k_f(t)$. $R$ and $\alpha$ denote the universal gas constant and the charge transfer coefficient, respectively. $U^{\pm}(.)$ and $i_0^{\pm}(t)$ are open-circuit potential and exchange current density, respectively. $t_{\mathrm{c}}^0$ is the transference number of ions, and $c_{\mathrm{ss}}^{\pm} = c_{\mathrm{s}}^{\pm}(t,R_{\mathrm{s}}^{\pm})$. $R_f^{\pm}$ and $\kappa$ are the solid-electrolyte interphase film resistance and the conductivity of electrolyte, respectively. The exchange current density is defined as

$$i_0^{\pm}(t) = r_{\mathrm{eff}}^{\pm}(T(t))\left[c_{\mathrm{ss}}^{\pm}(t)\right]^{\alpha}\left[c_{\mathrm{e},0}\left(c_{\mathrm{s}}^{\pm,\max}-c_{\mathrm{ss}}^{\pm}(t)\right)\right]^{\alpha}, \tag{14}$$

where $r_{\mathrm{eff}}^{\pm}(T(t))$ represents the effective reaction rate in the solid phase.

### D. Temperature dynamic

The internal averaged temperature $T(t)$ satisfies [10]:

$$\begin{aligned} \rho^{\mathrm{avg}}c_p\frac{\mathrm{d}T}{\mathrm{d}t}(t) = &\ h_{\mathrm{cell}}(T_{\mathrm{amb}}(t)-T(t))-I(t)V(t) \\ &+I(t)\Big\{U^{+}\left(\bar{c}_{\mathrm{s}}^{+}(t),T(t)\right)-U^{-}\left(\bar{c}_{\mathrm{s}}^{-}(t),T(t)\right) \\ &-T(t)\left[\frac{\partial U^{+}\left(\bar{c}_{\mathrm{s}}^{+}(t),T(t)\right)}{\partial T}-\frac{\partial U^{-}\left(\bar{c}_{\mathrm{s}}^{-}(t),T(t)\right)}{\partial T}\right]\Big\} \\ &+R_{\mathrm{c}}I(t)^2,\ t>0, \end{aligned} \tag{15}$$

$$T(0) = T_{\mathrm{amb}}(0), \tag{16}$$

where $T_{\text{amb}}(t)$ is the ambient temperature and $\bar{c}_{\text{s}}^{\pm}(t)$ are the average solid concentrations as:

$$\bar{c}_{\text{s}}^{\pm}(t) = \frac{3}{\left(R_{\text{s}}^{\pm}\right)^3} \int_0^{R_{\text{s}}^{\pm}} r_{\text{s}}^2 c_{\text{s}}^{\pm}(t, r_{\text{s}})\, \mathrm{d}r_{\text{s}}. \tag{17}$$

To eliminate the dependency of battery parameters on the internal averaged temperature $T(t)$ the following concentration is considered:

**Assumption 1.** *$U^{\pm}(c_{ss}^{\pm}(t), T(t))$ and $i_0^{\pm}(c_{ss}^{\pm}(t), T(t))$ are treated as independent of the concentrations, and their dependence on temperature $T(t)$ is approximated by a dependence on the ambient temperature $T_{amb}(t)$, as follows:*

$$\check{U}_1^{\pm}(t) \triangleq U^{\pm}\left(c_{\text{ss}}^{\pm}(t), T_{\text{amb}}(t)\right), \tag{18}$$
$$\check{U}_2^{\pm}(t) \triangleq U^{\pm}\left(\bar{c}_{\text{s}}^{\pm}(t), T_{\text{amb}}(t)\right), \tag{19}$$
$$\check{i}_0^{\pm}(t) \triangleq i_0^{\pm}(T_{\text{amb}}(t)), \tag{20}$$

*where the subscript 1 in $\check{U}$ indicates that $U^{\pm}(\cdot, T(t))$ is approximated using the surface concentration $c_{\text{ss}}^{\pm}(t) \triangleq c_{\text{s}}^{\pm}(t, R_s^{\pm})$, whereas subscript 2 refers to its approximation based on the averaged concentration $\bar{c}_{\text{s}}^{\pm}(t)$.*

In addition, the temperature-dependent parameter $R_\Omega(T(t))$ is replaced with an ambient temperature-dependent parameter, i.e., $\check{R}_\Omega(t) \triangleq R_\Omega(T_{\text{amb}}(t))$. For designing this observer, the required measurement is $c_{\text{e}}^{\pm}(t, 0^{\pm})$, which can be measured as detailed in the following remarks.

**Remark 1.** *The electrolyte lithium concentration at the terminal boundaries, $c_e^{\pm}(t, 0^{\pm})$, is difficult to measure directly. Therefore, correlated measurable quantities such as electrolyte resistance, diffusion coefficient, and conductivity can be used for its estimation. These quantities can be obtained through localized Electrochemical Impedance Spectroscopy (EIS), and subsequently used to determine $c_e^{\pm}(t, 0^{\pm})$. Detailed explanation can be found in [5]. EIS is an offline technique that typically requires about 2–3 minutes to complete each measurement [11]. Integrating event-triggered mechanisms into the observer is considered as a future work to address the offline nature of EIS.*

By substituting the voltage function (13) into (15) and applying Assumption 1, the internal average temperature dynamics (15) can be simplified and expressed as follows:

$$\rho^{\text{avg}} c_{\text{p}} \frac{\mathrm{d}\check{T}}{\mathrm{d}t}(t) = \chi(t)\check{T}(t) + \omega(t), \tag{21}$$

where

$$\begin{aligned}
\chi(t) = &-h_{\text{cell}} + \frac{R}{\alpha F} I(t) \left[ \sinh^{-1}\left( \frac{I(t)}{2\check{i}_0^{+}(t) a^{+} L^{+}} \right) \right. \\
&+ \sinh^{-1}\left( \frac{I(t)}{2\check{i}_0^{-}(t) a^{-} L^{-}} \right) \\
&\left. - I(t) \left[ \frac{\partial \check{U}_2^{+}}{\partial T}(t) - \frac{\partial \check{U}_2^{-}}{\partial T}(t) \right] \right], \\
\omega(t) = &\, h_{\text{cell}} T_{\text{amb}}(t) - \\
&\left( \check{R}_\Omega + \frac{L^{\text{sep}}}{A\check{\kappa}_{\text{e}}^{\text{sep}}(t)} + \frac{L^{+}}{2A\check{\kappa}_{\text{e}}^{+}(t)} + \frac{L^{-}}{2A\check{\kappa}_{\text{e}}^{-}(t)} \right) I(t)^2 \\
&- I(t)\left[\check{U}_1^{+}(t) - \check{U}_1^{-}(t)\right] + I(t)\left[\check{U}_2^{+}(t) - \check{U}_2^{-}(t)\right] \\
&- \frac{2RT(1 - t_c^0)(1+\gamma)}{F} \ln\left( \frac{c_e^{+}(t, 0^{+})}{c_e^{-}(t, 0^{-})} \right) I(t).
\end{aligned} \tag{22}$$

In (22), electrolyte-related terms are incorporated, making it distinct and more precise compared to Equation 24 in [3], which satisfies the following equation:

$$\begin{aligned}
\check{T}(t) = &\, \check{T}(0) e^{\frac{1}{\rho^{\text{avg}} C_p} \int_0^t \chi(\tau) d\tau} \\
&+ \frac{1}{\rho^{\text{avg}}\, C_{\text{P}}} \int_0^t e^{\frac{1}{\rho^{\text{avg}} C_{\text{P}}} \int_0^{t-\tau} \chi(\sigma)\mathrm{d}\sigma} \omega(\tau)\mathrm{d}\tau.
\end{aligned} \tag{23}$$

Afterward, in the equations involving $T(t)$, it is replaced by the simplified temperature $\check{T}(t)$ defined in (23). At this stage, the internal averaged temperature becomes a time-varying, concentration-independent function that depends only on time. Consequently, by using $\check{T}(t)$, the solid-phase diffusion coefficients $D_{\text{e}}^{+,\text{eff}}(\check{T}(t))/\varepsilon_{\text{e}}^{+}$ and electrolyte-phase diffusion coefficients $D_{\text{s}}^{+}(\hat{T}(t))/r_{\text{s}}^2$ become known.

## III. Electrolyte-phase lithium concentration observers

In the following section, electrolyte-phase observers incorporating temperature effects on the electrolyte diffusion coefficient are presented.

### A. Electrolyte observer for negative electrode

Unlike the previous approach in [8], where the system was first normalized to facilitate observer design, in this study normalization cannot be applied because the diffusion coefficient $D_{\text{e}}^{+,\text{eff}}(\check{T}(t))/\varepsilon_{\text{e}}^{+}$ is no longer constant. This variation, along with the inclusion of temperature effects, makes the observer design more challenging. The proposed observer for the electrolyte lithium concentration in the negative electrode (6), (9) and (10) is designed as follows:

$$\begin{aligned}
\frac{\partial \hat{c}_{\text{e}}^{-}}{\partial t}(t, x) = &\frac{D_{\text{e}}^{-,\text{eff}}(\check{T}(t))}{\varepsilon_{\text{e}}^{-}} \frac{\partial^2 \hat{c}_{\text{e}}^{-}(t, x)}{\partial x^2} + \frac{(1 - t_c^0)}{\varepsilon_{\text{e}}^{-} F L^{-}} I(t) \\
&+ k_1^{-}(t, x)(c_{\text{e}}^{-}(t, 0^{-}) - \hat{c}_{\text{e}}^{-}(t, 0^{-})),
\end{aligned} \tag{24}$$

$$\frac{\partial \hat{c}_{\text{e}}^{-}}{\partial x}(t, 0^{-}) = k_{10}^{-}(c_{\text{e}}^{-}(t, 0^{-}) - \hat{c}_{\text{e}}^{-}(t, 0^{-})), \tag{25}$$

$$\frac{\partial \hat{c}_{\text{e}}^{-}}{\partial x}(t, L^{-}) = \frac{-\hat{c}_{\text{e}}^{-}(t, L^{-})}{P^{*}}, \tag{26}$$

where $k_1^{-}(t, x)$ and $k_{10}^{-}$ are the observer gains determined such that $\hat{c}_{\text{e}}^{-}(t, x)$ converges to $c_{\text{e}}^{-}(t, x)$ as time

approaches infinity. The dynamics of the state estimation error $\tilde{c}_{\mathrm{e}}^{-}(t,x) = c_{\mathrm{e}}^{-}(t,x) - \hat{c}_{\mathrm{e}}^{-}(t,x)$ are given by:

$$\frac{\partial \tilde{c}_{\mathrm{e}}^{-}}{\partial t}(t,x) = \frac{D_{\mathrm{e}}^{-,\mathrm{eff}}(\check{T}(t))}{\varepsilon_{\mathrm{e}}^{-}} \frac{\partial^2 \tilde{c}_{\mathrm{e}}^{-}}{\partial x^2}(t,x) - k_1^{-}(t,x)\tilde{c}_{\mathrm{e}}^{-}(t,0^{-}), \tag{27}$$

$$\frac{\partial \tilde{c}_{\mathrm{e}}^{-}}{\partial x}(t,0^{-}) = -k_{10}^{-}\tilde{c}_{\mathrm{e}}^{-}(t,0^{-}), \tag{28}$$

$$\frac{\partial \tilde{c}_{\mathrm{e}}^{-}}{\partial x}(t,L^{-}) = \frac{-\tilde{c}_{\mathrm{e}}^{-}(t,L^{-})}{P^{*}}. \tag{29}$$

The following invertible backstepping transformation is:

$$\tilde{c}_{\mathrm{e}}^{-}(t,x) = \tilde{w}^{-}(t,x) - \int_0^x k^{-}(t,x,y)\tilde{w}^{-}(t,y)\,dy, \tag{30}$$

and the following exponentially stable target system is considered:

$$\frac{\partial \tilde{w}^{-}}{\partial t}(t,x) = \frac{D^{-,\mathrm{eff}}(\check{T}(t))}{\varepsilon_{\mathrm{e}}^{-}} \frac{\partial^2 \tilde{w}^{-}}{\partial x^2}(t,x) + \lambda^{-}\tilde{w}^{-}(t,x), \tag{31}$$

$$\frac{\partial \tilde{w}^{-}}{\partial x}(t,0^{-}) = \frac{1}{2}\lambda^{-}\tilde{w}^{-}(t,0^{-}), \tag{32}$$

$$\frac{\partial \tilde{w}^{-}}{\partial x}(t,L^{-}) = -\frac{1}{2}\tilde{w}^{-}(t,L^{-}), \tag{33}$$

where $\lambda^{-} < \min_{t\geq 0}\left\{D_{\mathrm{e}}^{-}(\check{T}(t))\right\} / (4\varepsilon_{\mathrm{e}}^{-})$ is an adjustable parameter determining the convergence rate of the observer to the system. The kernel function is derived as follows:

$$\frac{\partial k^{-}}{\partial t}(t,x,y) = \frac{D_{\mathrm{e}}^{-,\mathrm{eff}}(\check{T}(t))}{\varepsilon_{\mathrm{e}}^{-}} \left[\frac{\partial^2 k^{-}(t,x,y)}{\partial x^2} - \frac{\partial^2 k^{-}(t,x,y)}{\partial y^2}\right] - \lambda^{-}k^{-}(t,x,y), \tag{34}$$

$$k^{-}(t,0,y) = 0, \tag{35}$$

$$k^{-}(t,x,x) = \frac{\varepsilon_{\mathrm{e}}^{-}}{2D_{\mathrm{e}}^{-,\mathrm{eff}}(\check{T}(t))}\lambda^{-}x. \tag{36}$$

The kernel function is defined over the domain $\mathcal{T} = \{(t,x,y); 0 \leq t \leq t_{\max}, 0 \leq y \leq x \leq 1\}$, where $t_{\max}$ represents a suitable finite time ensuring the regularity conditions hold. The kernel function can be solved piecewise using the successive approximation method in Section 4.4 [12]. Observer gains should be selected as:

$$k_1^{-}(t,r) = \frac{D_{\mathrm{e}}^{-}(\check{T}(t))}{\varepsilon_{\mathrm{e}}^{-}}\left(k_y(t,x,0) - \frac{1}{2}k(t,x,0)\right), \tag{37}$$

$$k_{10}^{-}(t) = -\frac{1}{2}\lambda^{-}. \tag{38}$$

**Theorem 1.** *Consider the electrolyte lithium concentration in the positive electrode* (6)*,* (9) *and* (10)*, along with the proposed state observer* (24)-(26)*. Under Assumption 1, if*

$$\lambda^{-} < \min_{t\geq 0}\left\{D_{\mathrm{e}}^{-}(\check{T}(t))\right\} / \left(4\varepsilon_{\mathrm{e}}^{-}\right),$$

*then for any initial condition, the observer error system* (27)-(29) *is exponentially stable. This implies that the states of the designed observer* (24)-(26) *converges to the states of the system* (6)*,* (9) *and* (10)*.*

*Proof:* The stability of the observers will be proved following the procedure in [8], with the key difference that the boundary condition of the target system at $L^{-}$ is set to be nonzero to prevent the observer gain $k_{10}^{-}$ from becoming zero. The reason for this choice is that differentiating the transformations (30) and then substituting $x = 0$, leads to:

$$\frac{\partial \tilde{c}_{\mathrm{e}}^{-}}{\partial x}(t,x) = \frac{\partial \tilde{w}_{\mathrm{e}}}{\partial x}(t,x) - k^{-}(t,x,x)\tilde{w}(t,x) \tag{39}$$

$$- \int_0^x k_x^{-}(t,x,x)\tilde{w}(t,y)dy. \tag{40}$$

By using (68) and substituting $x = 0^{-}$ into (40), the following equation is obtained:

$$-k_{10}^{-}\tilde{c}_{\mathrm{e}}(t,0^{-}) = \frac{\partial \tilde{w}}{\partial x}(t,0^{-}).$$

As can be observed, if the boundary condition of the target system $\frac{\partial \tilde{w}}{\partial x}(t,0^{-})$ is set to zero, as in [8], then the observer gain $k_{10}^{-}$ must also be zero. To avoid it, in this study the boundary condition of the target system is defined as nonzero, as specified in (32).

### *B. Electrolyte observer for positive electrode*

The designed observer for the electrolyte lithium concentration in the positive electrode (8), (9) and (11) is expressed as follows:

$$\frac{\partial \hat{c}_{\mathrm{e}}^{+}}{\partial t}(t,x) = \frac{D_{\mathrm{e}}^{+,\mathrm{eff}}(\check{T}(t))}{\varepsilon_{\mathrm{e}}^{+}} \frac{\partial^2 \hat{c}_{\mathrm{e}}^{+}}{\partial x^2}(t,x) + \frac{(1-t_c^0)}{\varepsilon_{\mathrm{e}}^{-}FL^{-}}I(t) + k_1^{+}(t,x)(c_{\mathrm{e}}^{+}(t,0^{+}) - \hat{c}_{\mathrm{e}}^{+}(t,0^{+})), \tag{41}$$

$$\frac{\partial \hat{c}_{\mathrm{e}}^{+}}{\partial x}(t,0^{+}) = k_{10}^{+}(c_{\mathrm{e}}^{+}(t,0^{+}) - \hat{c}_{\mathrm{e}}^{-}(t,0^{+})), \tag{42}$$

$$\frac{\partial \hat{c}_{\mathrm{e}}^{+}}{\partial x}(t,L^{+}) = \frac{\hat{c}_{\mathrm{e}}^{+}(t,L^{+})}{L^{\mathrm{sep}} - P^{*}}, \tag{43}$$

where $k_1^{+}(t,x)$ and $k_{10}^{+}$ are observer gains designed to guarantee that $\hat{c}_{\mathrm{e}}^{+}(t,x)$ converges to $c_{\mathrm{e}}^{+}(t,x)$ as time approaches infinity. State estimation error $\tilde{c}_{\mathrm{e}}^{+}(t,x) = c_{\mathrm{e}}^{+}(t,x) - \hat{c}_{\mathrm{e}}^{+}(t,x)$ is obtained as:

$$\frac{\partial \tilde{c}_{\mathrm{e}}^{+}}{\partial t}(t,x) = \frac{D_{\mathrm{e}}^{+,\mathrm{eff}}(\check{T}(t))}{\varepsilon_{\mathrm{e}}^{+}} \frac{\partial^2 \tilde{c}_{\mathrm{e}}^{+}}{\partial x^2}(t,x) - k_1^{+}(t,x)\tilde{c}_{\mathrm{e}}^{+}(t,0^{+}), \tag{44}$$

$$\frac{\partial \tilde{c}_{\mathrm{e}}^{+}}{\partial x}(t,0^{+}) = -k_{10}^{+}\tilde{c}_{\mathrm{e}}^{+}(t,0^{+}), \tag{45}$$

$$\frac{\partial c_{\mathrm{e}}^{+}}{\partial x}(t,L^{+}) = \frac{c_{\mathrm{e}}^{+}(t,L^{+})}{L^{\mathrm{sep}} - P^{*}}. \tag{46}$$

By finding the following invertible transformation:

$$\tilde{c}_{\mathrm{e}}^{+}(t,x) = \tilde{w}^{+}(t,x) - \int_0^x k^{+}(t,x,y)\tilde{w}^{+}(t,y)dy, \tag{47}$$

where $\tilde{\omega}^+(t,x)$ satisfies the following exponentially stable target system:

$$\frac{\partial \tilde{w}^+}{\partial t}(t,x) = \frac{D_{\mathrm{e}}^{+,\mathrm{eff}}(\check{T}(t))}{\varepsilon_{\mathrm{e}}^+}\frac{\partial^2 \tilde{w}^+}{\partial x^2}(t,x) + \lambda^+ \tilde{w}^+(t,x), \tag{48}$$

$$\frac{\partial \tilde{w}^+}{\partial x}(t,0^+) = \frac{1}{2}\lambda^+ \tilde{w}^+(t,0^+), \tag{49}$$

$$\frac{\partial \tilde{w}^+}{\partial x}(t,L^+) = -\frac{1}{2}\tilde{w}^+(t,L^+), \tag{50}$$

where $\lambda^+ < \min_{t\geq 0}\left\{D_{\mathrm{e}}^+(T(t))\right\}/(4\varepsilon_{\mathrm{e}}^+)$ is an adjustable parameter determining the convergence rate of the observer to the system. Kernel function is derived as follows:

$$\frac{\partial k^+}{\partial t}(t,x,y) = \frac{D_{\mathrm{e}}^{+,\mathrm{eff}}(\check{T}(t))}{\varepsilon_{\mathrm{e}}^+}\left[\frac{\partial^2 k^+(t,x,y)}{\partial x^2} - \frac{\partial^2 k^+(t,x,y)}{\partial y^2}\right] \lambda^+ k^+(t,x,y), \tag{51}$$

$$k^+(t,0,y) = 0, \tag{52}$$

$$k^+(t,x,x) = \frac{\varepsilon_{\mathrm{e}}^+}{2D_{\mathrm{e}}^{+,\mathrm{eff}}(\check{T}(t))}\lambda^+ x. \tag{53}$$

Observer gains will be obtained as:

$$k_1^+(t,r) = \frac{D_{\mathrm{e}}^+(\check{T}(t))}{\varepsilon_{\mathrm{e}}^+}\left(k_y(t,x,0) - \frac{1}{2}k(t,x,0)\right), \tag{54}$$

$$k_{10}^+(t) = -\frac{1}{2}\lambda^+. \tag{55}$$

**Theorem 2.** *Consider the electrolyte lithium concentration in the positive electrode* (8)*,* (9) *and* (11)*, along with the proposed state observer* (41)–(43)*. Under Assumption 1, if*

$$\lambda^+ < \min_{t\geq 0}\left\{D_{\mathrm{e}}^+(\check{T}(t))\right\}/\left(4\varepsilon_{\mathrm{e}}^+\right),$$

*then, for any initial condition, observer error system* (44)-(46) *is exponentially stable. This implies that the states of the designed observer* (41)-(43) *converges to the states of the system* (8)*,* (9) *and* (11)*.*

*Proof:* The stability follows directly from Theorem 1. Since the procedure is identical, the detailed proof is omitted for brevity.

### C. Electrolyte observer for separator

Observer for the system within the separator is designed as follows:

$$\frac{\partial \hat{c}_{\mathrm{e}}^{\mathrm{sep}}}{\partial t}(t,x) = \frac{D_{\mathrm{e}}^{+,\mathrm{eff}}(\check{T}(t))}{\varepsilon_{\mathrm{e}}^+}\frac{\partial^2 \hat{c}_{\mathrm{e}}^{\mathrm{sep}}}{\partial x^2}(t,x) + k_1^{\mathrm{sep}}(t,x)\tilde{c}_{\mathrm{e}}^{\mathrm{sep}}(t,0^{\mathrm{sep}}), \tag{56}$$

$$\frac{\partial \hat{c}_{\mathrm{e}}^{\mathrm{sep}}}{\partial x}(t,0^{\mathrm{sep}}) = \frac{-L^-\hat{c}_{\mathrm{e}}^{\mathrm{sep}}(t,0^{\mathrm{sep}})}{P^*} - k_{10}^{\mathrm{sep}}\tilde{c}_{\mathrm{e}}^{\mathrm{sep}}(t,0^{\mathrm{sep}}), \tag{57}$$

$$\frac{\partial \hat{c}_{\mathrm{e}}^{\mathrm{sep}}}{\partial x}(t,L^{\mathrm{sep}}) = \frac{\hat{c}_{\mathrm{e}}^{\mathrm{sep}}(t,L^{\mathrm{sep}})}{L^{\mathrm{sep}}-P^*}, \tag{58}$$

where $\tilde{c}_{\mathrm{e}}^{\mathrm{sep}}(t,0^{\mathrm{sep}}) = c_{\mathrm{e}}^{\mathrm{sep}}(t,0^{\mathrm{sep}}) - \hat{c}_{\mathrm{e}}^{\mathrm{sep}}(t,0^{\mathrm{sep}})$. Observer gains are $k_1^{\mathrm{sep}}(t,x)$ and $k_{10}^{\mathrm{sep}}$. The separator observer operates in cascade with the electrolyte observers in the positive and negative electrodes, since its boundary terms $c_{\mathrm{e}}^{\mathrm{sep}}(t,0^{\mathrm{sep}}) = c_{\mathrm{e}}^-(t,L^-)$ and $c_{\mathrm{e}}^{\mathrm{sep}}(t,L^{\mathrm{sep}}) = c_{\mathrm{e}}^+(t,0^+)$ are obtained from the corresponding electrode observer estimates.

The dynamics of the state error $c_{\mathrm{e}}^{\mathrm{sep}}(t,0^{\mathrm{sep}}) = c_{\mathrm{e}}^{\mathrm{sep}}(t,L^-)$ are obtained as:

$$\frac{\partial \tilde{c}_{\mathrm{e}}^{\mathrm{sep}}}{\partial t}(t,x) = \frac{D_{\mathrm{e}}^{+,\mathrm{eff}}(\check{T}(t))}{\varepsilon_e^+}\frac{\partial^2 \tilde{c}_{\mathrm{e}}^{\mathrm{sep}}}{\partial x^2}(t,x) - k_1^{\mathrm{sep}}(t,x)\tilde{c}_{\mathrm{e}}^{\mathrm{sep}}(t,0^{\mathrm{sep}}), \tag{59}$$

$$\frac{\partial \tilde{c}_{\mathrm{e}}^{\mathrm{sep}}}{\partial x}(t,0^{\mathrm{sep}}) = \frac{-L^-\tilde{c}_{\mathrm{e}}^{\mathrm{sep}}(t,L^{\mathrm{sep}})}{P^*} - k_{10}^{\mathrm{sep}}\tilde{c}_{\mathrm{e}}^{\mathrm{sep}}(t,0^{\mathrm{sep}}), \tag{60}$$

$$\frac{\partial \tilde{c}_{\mathrm{e}}^{\mathrm{sep}}}{\partial x}(t,L^{\mathrm{sep}}) = \frac{\tilde{c}_{\mathrm{e}}^{\mathrm{sep}}(t,L^{\mathrm{sep}})}{L^{\mathrm{sep}}-P^*}. \tag{61}$$

Using the following invertible transformation:

$$\tilde{c}_{\mathrm{e}}^{\mathrm{sep}}(t,x) = \tilde{w}^-(t,x) - \int_0^x k^{\mathrm{sep}}(t,x,y)\tilde{w}(t,y)^{\mathrm{sep}}\,dy, \tag{62}$$

where $\tilde{\omega}^{\mathrm{sep}}(t,x)$ satisfies the following exponentially stable target system:

$$\frac{\partial \tilde{w}^{\mathrm{sep}}}{\partial t}(t,x) = \frac{D_{\mathrm{e}}^{^{\mathrm{sep}},\mathrm{eff}}(\check{T}(t))}{\varepsilon_e^{\mathrm{sep}}}\frac{\partial^2 \tilde{w}^{\mathrm{sep}}}{\partial x^2}(t,x) + \lambda^{\mathrm{sep}}\tilde{w}^{\mathrm{sep}}(t,x), \tag{63}$$

$$\frac{\partial \tilde{w}^{\mathrm{sep}}}{\partial x}(t,0^{\mathrm{sep}}) = \frac{1}{2}\lambda^{\mathrm{sep}}\tilde{w}^{\mathrm{sep}}(t,0^{\mathrm{sep}}), \tag{64}$$

$$\frac{\partial \tilde{w}^{\mathrm{sep}}}{\partial x}(t,L^{\mathrm{sep}}) = -\frac{1}{2}\tilde{w}^{\mathrm{sep}}(t,L^{\mathrm{sep}}), \tag{65}$$

where $\lambda^{\mathrm{sep}} < \min_{t\geq 0}\left\{D_{\mathrm{e}}^{\mathrm{sep}}(\check{T}(t))\right\}/\left(4\varepsilon_{\mathrm{e}}^{\mathrm{sep}}\right)$ is an adjustable parameter determining the convergence rate of the observer to the system. The kernel function is derived as follows:

$$\frac{\partial k^{\mathrm{sep}}}{\partial t}(t,x,y) = \frac{D_e^{\mathrm{sep},\mathrm{eff}}(\check{T}(t))}{\varepsilon_{\mathrm{e}}^{\mathrm{sep}}}\times \left(\frac{\partial^2 k^{\mathrm{sep}}(t,x,y)}{\partial x^2} - \frac{\partial^2 k^{\mathrm{sep}}(t,x,y)}{\partial y^2}\right) - \lambda^{\mathrm{sep}}k^{\mathrm{sep}}(t,x,y), \tag{66}$$

$$k^{\mathrm{sep}}(t,0,y) = 0, \tag{67}$$

$$k^{\mathrm{sep}}(t,x,x) = \frac{\varepsilon_{\mathrm{e}}^{\mathrm{sep}}}{2D_{\mathrm{e}}^{\mathrm{sep},\mathrm{eff}}(\check{T}(t))}\lambda^{\mathrm{sep}}x, \tag{68}$$

where observer gains are chosen as:

$$k_1^{\mathrm{sep}}(t,r) = \frac{D_{\mathrm{e}}^-(\check{T}(t))}{\varepsilon_{\mathrm{e}}^-}\left(k_y(t,x,0) - \frac{1}{2}k(t,x,0)\right), \tag{69}$$

$$k_{10}^{\mathrm{sep}}(t) = -\frac{1}{2}\lambda^{\mathrm{sep}}. \tag{70}$$

**Theorem 3.** *Consider the electrolyte lithium concentration in the separator* (7)*,* (10) *and* (11)*, along with the proposed state observer* (56)–(58)*. Under Assumption 1, if*

$$\lambda^{sep}m < \min_{t\geq 0}\left\{D_{\mathrm{e}}^{sep}(\check{T}(t))\right\}/\left(4\varepsilon_{\mathrm{e}}^{sep}\right),$$

*then, for any initial condition, the observer error system* (59)-(61) *is exponentially stable. This implies that the states of the designed observer* (56)-(58) *converges to the states of the system* (7)*,* (10) *and* (11)*.*

*Proof:* The stability can be proved following the similar procedure explained for Theorem 1.

## IV. Solid-phase observer design

The design of the solid-phase observer requires the solid-phase lithium concentration at the boundary. The solid-phase observer that accounts for the temperature dependence of the solid-phase diffusion coefficient was previously designed in [3]. However, in this study, the boundary value of the surface concentration $c_{\mathrm{ss}}^{+}(t)$ is obtained using a more accurate scheme, as explained below. The positive electrode concentration at the boundary can be obtained through the inversion of the output function, by considering the following assumption:

**Assumption 2.** *Functions $I(t)$, $U^{\pm}(\cdot, T(t))$ and $V(t)$ are considered as piecewise analytic [3].*

The SPM voltage function is simplified as [3]:

$$V(t) = h_0(t, c_{\mathrm{ss}}^{+}(t), I(t)), \tag{71}$$

and its inversion $c_{\mathrm{ss}}^{+} = h_0(t, V(t), I(t))$ can be used to obtain $c_{\mathrm{ss}}^{+}(t)$. Whereas, this study employs a more comprehensive SPMe voltage function (13) compared with [3], which incorporates electrolyte concentration terms, expressed as:

$$V(t) = h_1\left(t, c_{\mathrm{ss}}^{+}(t), c_{\mathrm{e}}^{\pm}(t, 0^{\pm}), I(t)\right). \tag{72}$$

As detailed in Remark 1, the electrolyte lithium concentration at the boundaries $c_{\mathrm{e}}^{\pm}(t, 0^{\pm})$ can be determined indirectly through EIS measurement. Consequently, with access to $c_{\mathrm{e}}^{\pm}(t, 0^{\pm})$ and the measured voltage $V(t)$, a more precise value for $c_{\mathrm{ss}}^{+}(t)$ can be obtained compared to inverting (71).

$$c_{\mathrm{ss}}^{+}(t) = h_2\left(t, V(t), c_{\mathrm{e}}^{\pm}(t, 0^{\pm}), I(t)\right). \tag{73}$$

Using $c_{\mathrm{ss}}^{+}(t)$, obtained through the inversion of the output function, following observer is designed for the original system (1)-(4) as follows [3]:

$$\begin{aligned}\frac{\partial \hat{c}_{\mathrm{s}}^{+}}{\partial t}(t, r_{\mathrm{s}}) &= \frac{D_{\mathrm{s}}^{+}(\hat{T}(t))}{r_{\mathrm{s}}^{2}} \frac{\partial}{\partial r_{\mathrm{s}}}\left[r_{\mathrm{s}}^{2} \frac{\partial \hat{c}_{\mathrm{s}}^{+}}{\partial r_{\mathrm{s}}}(t, r_{\mathrm{s}})\right] \\ &\quad + p_1(t, r_{\mathrm{s}})\left(c_{\mathrm{ss}}^{+}(t) - \hat{c}_{\mathrm{ss}}^{+}(t)\right), \end{aligned} \tag{74}$$

$$\frac{\partial \hat{c}_{\mathrm{s}}^{+}}{\partial t}(t, 0) = 0, \tag{75}$$

$$\begin{aligned}\frac{\partial \hat{c}_{\mathrm{s}}^{+}}{\partial r}(t, R_{\mathrm{s}}) &= \frac{I(t)}{D_{\mathrm{s}}^{+}(\hat{T}(t)) a^{+} F L^{+}} \\ &\quad + p_{10}(t)\left(c_{\mathrm{ss}}^{+}(t) - \hat{c}_{\mathrm{ss}}^{+}(t)\right), \end{aligned} \tag{76}$$

where $p_1(t, r)$ and $p_{10}$ are the observer gains determined as:

$$p_1(t, r) = -\frac{D_{\mathrm{s}}^{+}(\check{T}(t))}{\left(R_{\mathrm{s}}^{+}\right)^{2} r}\left(p_l(t, r, 1) + \frac{1}{2} p(t, r, 1)\right), \tag{77}$$

$$p_{10}(t) = \frac{3}{2R_{\mathrm{s}}^{+}} - \frac{1}{2D_{\mathrm{s}}^{+}(\check{T}(t)) R_{\mathrm{s}}^{+}} \lambda_{\mathrm{s}}, \tag{78}$$

where $p(t, r, l)$ is the solution of the kernel function and $\lambda_{\mathrm{s}}$ is a free parameter satisfying $\lambda_{\mathrm{s}} < \frac{1}{4\left(R_{\mathrm{s}}^{-}\right)^{2}} \min_{t \geq 0}\left\{D_{\mathrm{s}}^{+}(\check{T}(t))\right\}$, elaborated in [3].

**Theorem 4.** *Under Assumptions 1 and 2, for $t \in [0, t_{max}]$ if*

$$\lambda_s < \frac{1}{4\left(R_{\mathrm{s}}^{+}\right)^{2}} \min_{t \geq 0}\left\{D_{\mathrm{s}}^{+}(\check{T}(t))\right\},$$

*then for any initial value, the states of the observer* (74)-(76) *converges to the states of the system* (1)-(4).

*Proof:* The stability proof can be found in the proof of Lemma 2 in [3].

## V. Conclusion

This paper presented a state estimation approach for the SPMe-T model, which accounts for the temperature dependence of the diffusion coefficient in both the solid phase and the electrolyte phase. The SPMe-T model improves accuracy by incorporating temperature effects on the diffusion coefficient. Closed-loop PDE backstepping observers were designed to estimate the lithium-ion concentration in the electrolyte and solid phases. Conducting validation of the designed observers and comparing their results with ongoing work is planned for future work. Using a more detailed temperature model [13] instead of the internal averaged model is another potential direction for future work.

## References


[1] D. Zhang, S. Park, L. D. Couto, V. Viswanathan, and S. J. Moura, "Beyond battery state of charge estimation: Observer for electrode-level state and cyclable lithium with electrolyte dynamics," *IEEE Transactions on Transportation Electrification*, vol. 9, no. 4, pp. 4846–4861, 2022.

[2] S. J. Moura, N. A. Chaturvedi, and M. Krstić, "Adaptive Partial Differential Equation Observer for Battery State-of-Charge/State-of-Health Estimation Via an Electrochemical Model," *Journal of Dynamic Systems, Measurement, and Control*, vol. 136, no. 1, pp. 011–015, 2014.

[3] S.-X. Tang, L. Camacho-Solorio, Y. Wang, and M. Krstic, "State-of-charge estimation from a thermal–electrochemical model of lithium-ion batteries," *Automatica*, vol. 83, pp. 206–219, 2017.

[4] S. J. Moura, F. B. Argomedo, R. Klein, A. Mirtabatabaei, and M. Krstic, "Battery state estimation for a single particle model with electrolyte dynamics," *IEEE Transactions on Control Systems Technology*, vol. 25, no. 2, pp. 453–468, 2016.

[5] S. Sepasiahooyi and S.-X. Tang, "State estimation for lithium-ion batteries based on electrolyte–electrode PDE observers," *Automatica*, vol. 183, p. 112568, 2026.

[6] L. He, Y. Wang, Y. Wei, M. Wang, X. Hu, and Q. Shi, "An adaptive central difference kalman filter approach for state of charge estimation by fractional order model of lithium-ion battery," *Energy*, vol. 244, p. 122627, 2022.

[7] R. Klein, N. A. Chaturvedi, J. Christensen, J. Ahmed, R. Findeisen, and A. Kojic, "Electrochemical model based observer design for a lithium-ion battery," *IEEE Transactions on Control Systems Technology*, vol. 21, no. 2, pp. 289–301, 2012.

[8] S. Sepasiahooyi and S.-X. Tang, "Enhanced battery state estimation: Part 1-electrolyte lithium-ion concentration observer," in *2024 IEEE 63rd Conference on Decision and Control (CDC)*. IEEE, 2024, pp. 3422–3427.

[9] T. Tranter, R. Timms, T. Heenan, S. Marquis, V. Sulzer, A. Jnawali, M. Kok, C. Please, S. Chapman, P. Shearing *et al.*, "Probing heterogeneity in li-ion batteries with coupled multiscale models of electrochemistry and thermal transport using tomographic domains," *Journal of The Electrochemical Society*, vol. 167, no. 11, p. 110538, 2020.

[10] K. E. Thomas, J. Newman, and R. M. Darling, "Mathematical modeling of lithium batteries," in *Advances in lithium-ion batteries*. Springer, 2002, pp. 345–392.

[11] A. C. Lazanas and M. I. Prodromidis, "Electrochemical impedance spectroscopy a tutorial," *ACS Measurement Science Au*, 2023.

[12] M. Krstic and A. Smyshlyaev, *Boundary control of PDEs: A course on backstepping designs*. SIAM, 2008.

[13] P. Ferreira and S.-X. Tang, "Cascaded electrochemical-thermal modeling and temperature estimation for cylindrical li-ion batteries," *Journal of Energy Storage*, vol. 124, p. 116438, 2025.